Development of H-II Transfer Vehicle (HTV)-Design and Verification for Large Structure with a Wide Opening

HIDEFUMI KAWANO[*1]   **ATSUSHI KUNO**[*1]

TOSHIO NAKAMURA[*2]   **YOICHIRO MIKI**[*1]

With space shuttle operation now under way, the H-II Transfer Vehicle (HTV) is drawing attention for carrying cargoes to the International Space Station (ISS), particularly for transfer under non-pressurized space conditions. The HTV is the only carrier besides the Space Shuttle with this capacity. Designing and verifying a large structure with a wide opening to realize the above capacity is difficult but interesting.

1. Introduction

The H-II Transfer Vehicle (HTV) is launched by the H-II B rocket (enhanced-capacity H-II A) to deliver cargo to the ISS. The project is being conducted under the aegis of the Japan Aerospace Exploration Agency (JAXA), and Mitsubishi Heavy Industries, Ltd. (MHI) integrates the overall system design and manufacture the Pressurized Logistics Carrier (PLC) and Unpressurized Logistics Carrier (ULC) carrying cargo and the Propulsion Module (PM) generating thrust.

The HTV consists of four modules (**Fig. 1**). PLC and ULC modules carry a maximum 6 tons of cargo. The ULC has a wide opening for inserting and removing an exposed pallet to carry and detach cargo exposed to space. The Avionics Module (AM) and Propulsion Module (PM) can transfer PLC and ULC cargoes in space. They have a secondary structure carrying electrical and propulsion components. MHI present the basic HTV structural design concept and introduce large (wide) opening design and verification.

2. Primary structure design concept

2.1 Load conditions

Structural design of spacecrafts is generally evaluated by launch load, which is calculated by Coupled Load Analysis (CLA). Mathematical models of HTV and rocket are coupled for applying external force derived from rocket launch to calculate the transient satellite (spacecraft) response. CLA has been conducted four times based on HTV progress in development (mathematical model) specifications.

2.2 Structural design concept

The HTV Primary structure is designed based on the semi-monocoque concept (a bony framework of a stringer, skin, and frame).

The stringer operates under the severest axial compression load path and is located circumferentially in all modules with a common phase. The HTV Primary structure basically has 48 stringers in the circumference.

The skin withstands horizontal load (lateral acceleration). The skin supported at the periphery by the stringer and frame must withstand load against shear strength. Because of minimized weight requirements, the skin enables elastic buckling. After buckling, the skin forms a semi-tensional field to withstand lateral load. Permanent (residual strain) derived from buckling is not allowed. The area where the skin is connected to the stringer (effective width area) can transmit axial load.

The frame operates mainly as a stiffness member enabling load to be transmitted smoothly among stringers and skins. The frame must be designed to support stringers and peripheral skin boundaries to maintain overall HTV stiffness.
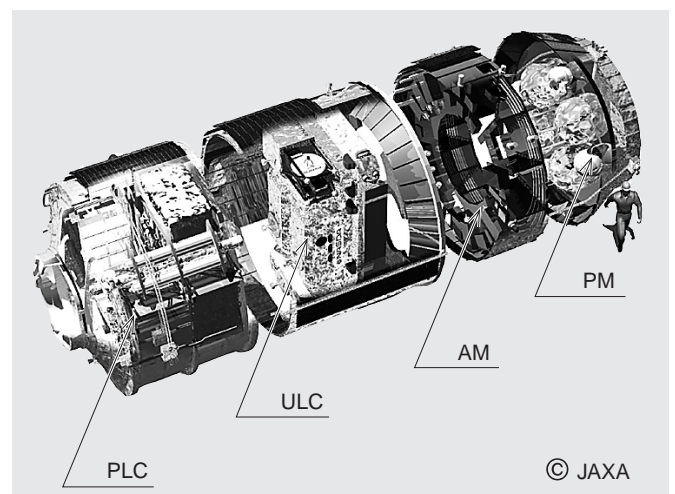

Fig. 1 HTV outline

3. ULC structural design

The ULC Primary structure is based on the semi-monocoque concept, but has a large opening (**Fig. 2**) for removing and inserting the exposed pallet. The opening requires that adjacent sections withstand severe load concentrations. In addition, HTV stiffness, especially torsional stiffness, gets extremely deteriorated.

This section focus on the design approach of strengthening for the opening. (Stiffness deterioration will be discussed in other paper).

3.1 Reinforcement specifications for the opening

Longerons with strength and stiffness ten times that of general stringers lie on both sides of the opening. Reinforced skins with three times thicker than the general ones are attached to both sides of longerons to prevent buckling. Reinforcement brackets (gussets) reduce stress at the corners of the opening.

3.2 Strength evaluation of opening

(1) Evaluation process

Basic strength evaluation process of the opening is shown in (a) - (d) in **Fig. 3**.

(a) Boundary displacement around the ULC opening is calculated by system model analysis under launch load (acceleration).

(b) Boundary displacement given by (a) is input to the detail zooming model as forced displacement to calculate stress distribution. This process makes a detailed evaluation model matching the structure around the opening regardless of computer capacity, and enables analysis evaluation in (c) and (d).

(c) Buckling eigenvalue analysis conducted by the zooming math model (b) confirmed that no buckling occurs in the stringer and skin around the opening under the defined load.
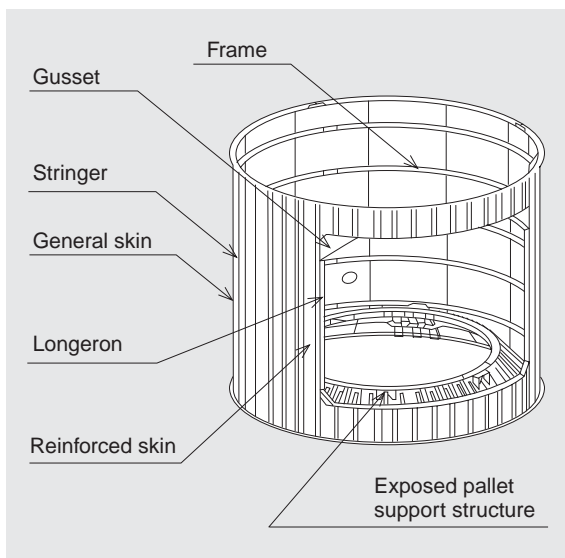
(d) It is confirmed by simulated large-deflection analysis (elastoplastic large deflection analysis: analysis tool ABAQUS) that the opening is not excessively deformed.

(2) Notes

In post-buckling design, math modeling of skin is represented by a shear panel that has no axial stiffness. The reinforced skin around the opening is modeled by a shell panel that has axial stiffness because buckling must be prevented. Both models use shear and shell panel for general skin, with the shear panel simulating post-buckling and the shell panel simulating pre-buckling.

Because of the asymmetric shape of the HTV due to the opening, the response behavior of HTV changes based on lateral load direction. Analysis is conducted by changing lateral load direction and strength is evaluated applying the severest load.
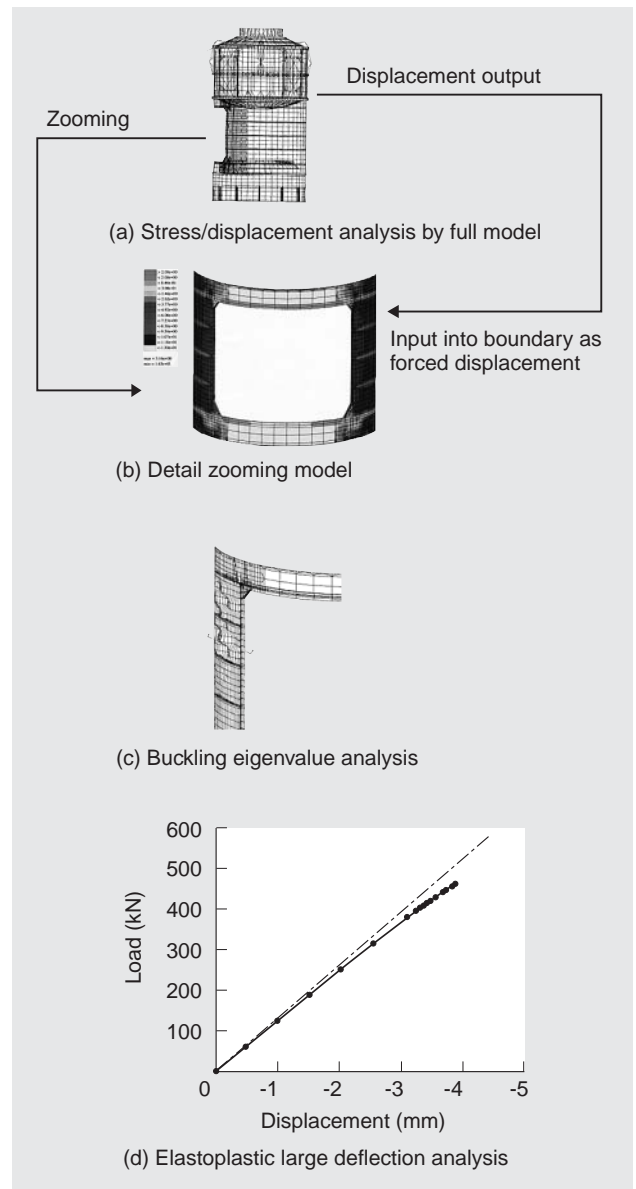

(a) Stress/displacement analysis by full model

(b) Detail zooming model

(c) Buckling eigenvalue analysis

(d) Elastoplastic large deflection analysis

Fig. 3 Strength evaluation of opening

Fig. 2 Outline of ULC primary structure

4. Strength test

4.1 Strength test configuration

Strength test specimens and test equipment setup are shown in **Fig. 4**. Load distribution in testing should be nearly equivalent to actual flight inertia load at launch. To simulate load distribution, test equipment gave axial and lateral loads independently to each plane of the PLC, exposed pallets and secondary AM structures (**Fig. 5**). Since the actual inertia load direction is arbitrary, two hydraulic jacks were set at right angles to make a vector of directions controlling lateral loading for each plane. (Four of tests were therefore conducted by changing load direction.) To observe skin buckling and residual deformation, skins were filmed by 4 video cameras and buckling data was obtained by image analysis.

4.2 Test results

All test specimens withstood loading conditions (limit/ultimate load), confirming the validity of structural design. In a typical case, lateral load was applied to the ULC opening.
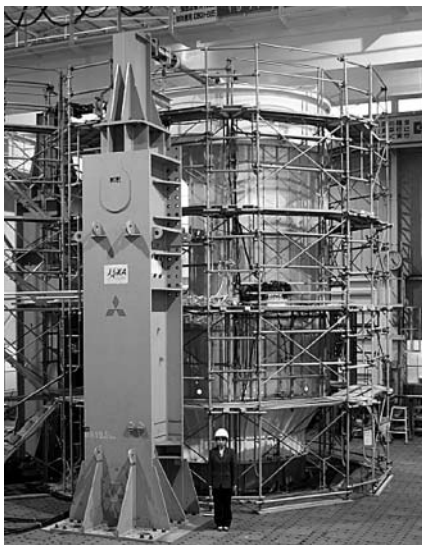
In **Figs. 6, 7 and 11**, the vertical axis shows the dimensionless number of the input load (F) divided by the evaluation load (FLMT).

Fig. 6 shows the relationship between shear strain and input load at maximum shear stress. Skin buckled at F/FLMT = 50%, but skin distributes load by forming a shear stress field, minimizing instability with strain increasing linearly until maximum input load. In load removal, strain decreases in almost the same way, leaving no residual strain.

Strain of longeron increases only slightly at F/FLMT= 50% during general buckling (Fig. 7), increasing proportionally to input load thereafter. No residual strain remains after load is removed.

Fig. 4 Strength test setup for primary structure
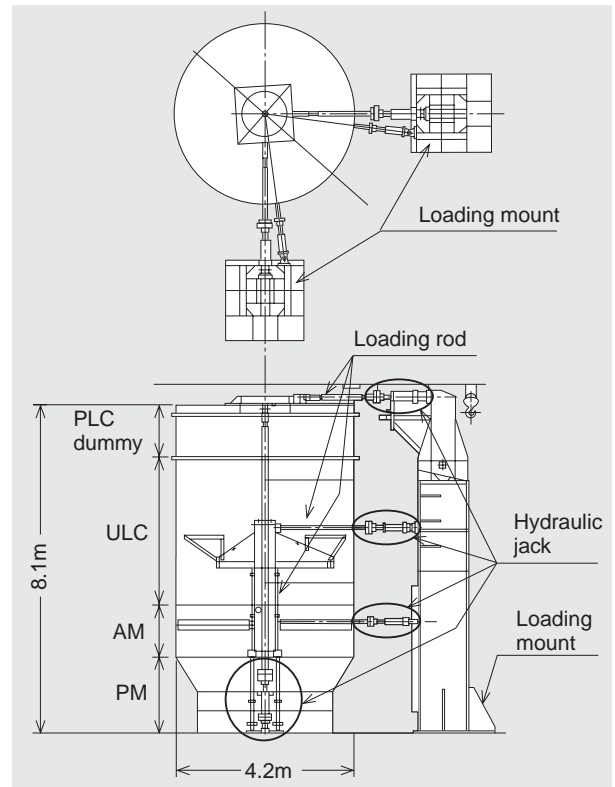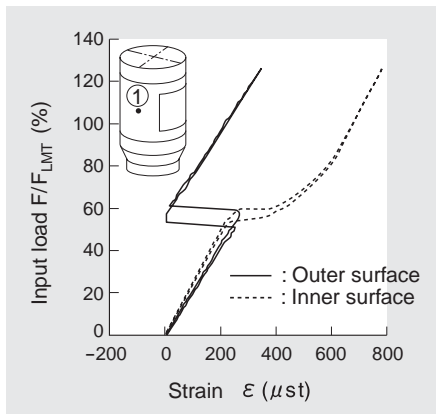

Fig. 5 Test specimens and equipments

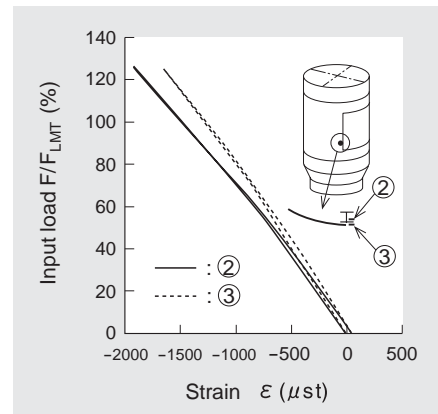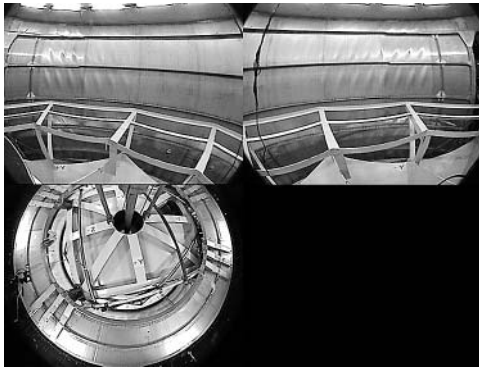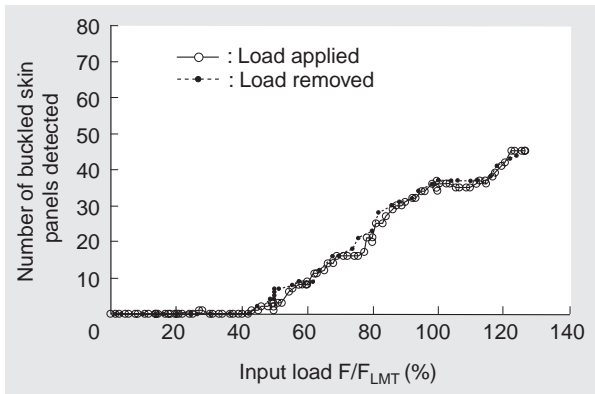**Fig. 6 Relationship between input load and skin panel strain**

Fig. 7 Relationship between input load and longeron strain

Fig. 8 Buckling generation of skin panel

Fig. 9 Relationship between input load and number of skin panels with buckling

Fig. 10 Analysis model (test configuration)
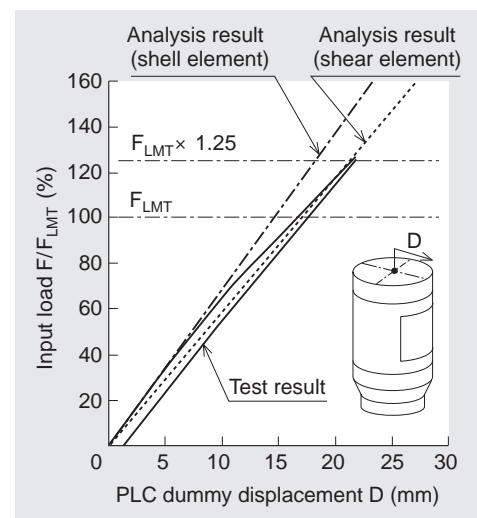
Fig. 11 Relationship between input load and PLC dummy displacement

Skin panels were filmed (**Fig. 8**), and image analysis was conducted to confirm buckling (**Fig. 9**). The number of panels buckling increased from F/FLMT = 50% and included 45 panels at maximum load. In load removal, this decreases equivalently. No residual deformation remained at any skin panel after load was removed.

4.3 Strength Analysis (Test model)

We confirmed the validity of the math analysis model with comparing test and analysis results.

Two models were prepared for skin panels molded as shell and shear (**Fig. 10**).

Comparison between test result and analysis result corresponding to item 4.2 is shown in **Fig. 11**. It shows the relationship between input load and lateral displacement of the PLC. The solid line shows test results, the dotted line shows analysis result for shear panels, and the dashed line shows analysis results for shell panels.

Displacement increases nonlinearly at F/FLMT = 50% point because the stiffness deteriorates due to the above skin buckling, with displacement increasing almost linearly after that. The comparison of test and analysis results shows that test results are similar to shell element results in lower load, while test results after skin panel buckling are between shell and shear element results. This shows that the analysis model in strength design is sufficiently accurate and strength evaluation is sufficiently conservative.
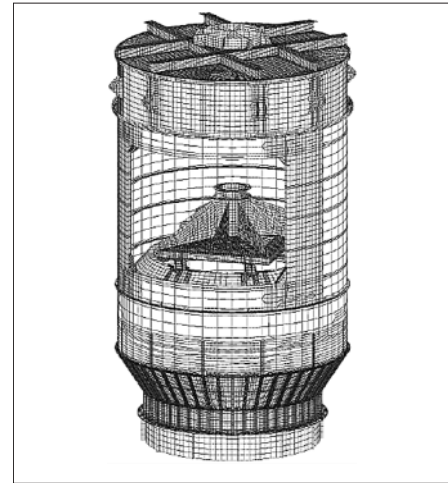
Residual displacement of approximately 1 mm remains after load removal (Fig. 11). This displacement is measured 8 000 mm above the test specimen's lower base, so when converted to an angle, it is extremely small, and is considered integrated slight slippage of each module interface because all modules are combined with fasteners.

5. Conclusion

This is, to our knowledge, the first time in domestic spacecraft development that a primary structure has such a wide opening. As a result of this technically challenging but successful development, the HTV became carried ULC cargo in orbit and has the potential to replace the Space Shuttle.

Hidefumi Kawano   Atsushi Kuno   Toshio Nakamura   Yoichiro Miki